

Supporting information
for

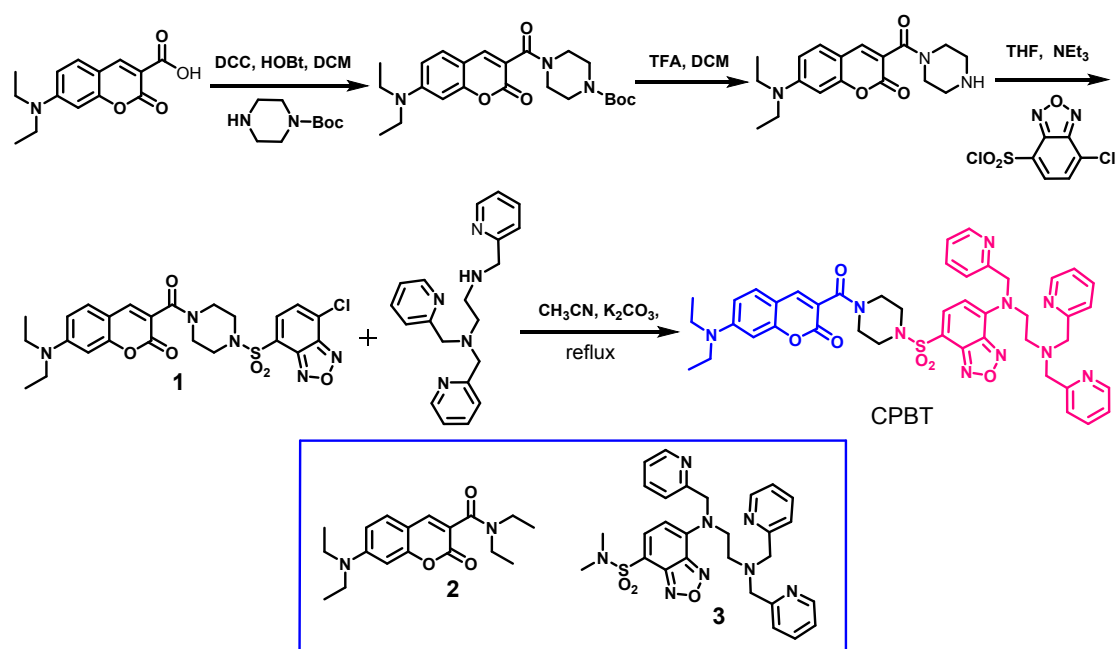
**A FRET-based fluorescent Zn²⁺ sensor: 3D ratiometric imaging,
flow cytometric tracking and cisplatin-induced Zn²⁺ fluctuation
monitoring**

Hongxia Xu,[‡] Chengcheng Zhu,[‡] Yuncong Chen,^{*} Yang Bai, Zhong Han, Shankun Yao, Yang Jiao, Hao Yuan, Weijiang He^{*} and Zijian Guo^{*}

1. Materials and General Methods

All chemicals were of analytical grade, the solvents were HPLC grade, and water obtained from a MilliQ system (>18.2 MΩ) was used in the spectroscopic study. ¹H- and ¹³C-NMR spectra were recorded on a Bruker DRX-400 using tetramethylsilane (TMS) as the internal reference. High-resolution mass spectra were obtained using an Agilent 6540 Q-TOF HPLC-MS spectrometer, and ESI-MS spectra were obtained using an LCQ Fleet electro-spray mass spectrometer (Thermo Finnigan). Fluorescence spectra were obtained on a FluoroMax-4 spectrofluorometer with a 5-nm slit for both excitation and emission. Absorption spectra were recorded on a Shimadzu UV-3100 spectrophotometer.

2. Synthesis and Characterization



Scheme S1. Synthesis of the CPBT sensor and chemical structures of reference compounds **2** and **3**, which are the analogues of donor and acceptor fluorophores in CPBT.

Synthesis of CPBT. Compound **1** (550 mg, 1.0 mmol), which was prepared using our previously reported procedure,¹ was mixed with TPEA (330 mg, 1.0 mmol) and K₂CO₃ (420 mg, 3.0 mmol) in 15 mL of CH₃CN with stirring, and the mixture was refluxed for 24 h. The reaction suspension was filtered and the filtrate was collected. After removing the solvent in vacuo, the residue was purified by column chromatography on a silica gel (CH₂Cl₂/MeOH, 8:1 v/v) to yield **CPBT** (450 mg, 53%). Mp: 93-94 °C. ¹H NMR (400 MHz, CD₃OD, ppm): δ 8.50-8.45 (m, 1H), 8.36 (ddd, *J* = 5.0, 1.7, 0.8 Hz, 2H), 7.86 (s, 1H), 7.76-7.70 (m, 2H), 7.67 (td, *J* = 7.7, 1.8 Hz, 2H), 7.52 (d, *J* = 7.8 Hz, 2H), 7.40 (d, *J* = 9.0 Hz, 1H), 7.28 (t, *J* = 7.2 Hz, 2H), 7.19 (ddd, *J* = 7.5, 5.0, 1.1 Hz, 2H), 6.74 (dd, *J* = 9.0, 2.5 Hz, 1H), 6.53 (d, *J* = 2.3 Hz, 1H), 6.10 (d, *J* = 8.5 Hz, 1H), 5.21 (s, 2H), 4.09 (m, 2H), 3.88 (s, 4H), 3.76 (m, 2H), 3.49 (m, 6H), 3.25 (s, 4H), 2.98 (t, *J* = 6.3 Hz, 2H), 1.20 (t, *J* = 7.1 Hz, 6H). ¹³C NMR (100 MHz, CDCl₃, ppm) δ 165.3, 159.4, 158.7, 157.5, 156.2, 152.0, 150.0, 149.3, 147.1, 145.9, 144.5, 142.5, 138.7, 137.2, 136.7, 130.1, 123.4, 122.8, 122.5, 121.1, 115.5, 109.6, 108.1, 107.8, 102.4, 97.0, 61.0, 58.5, 51.8, 50.9, 47.4, 46.3, 45.9, 45.1, 42.2, 12.5. ESI-HRMS (*m/z*, positive mode): calcd. 865.3220, observed 865.3214 for [M+Na]⁺.

Synthesis of compound 2. Thionyl chloride (3 mL) was mixed with 7-(diethylamino)-2-oxo -2H-chromene-3-carboxylic acid (100 mg, 0.38 mmol) and stirred for 4 h at room temperature. The reaction mixture was filtered and the solid was washed with cold ethanol. The collected solids and diethylamine (30 mg, 0.41 mmol) were dissolved in CH₂Cl₂ (10 mL) and stirred for 24 h. After removing the solvent in vacuo, the residue was purified by column chromatography on silica gel (CH₂Cl₂/ethyl acetate, 5:1 v/v) to yield compound **2** (52 mg, 43.8%). ¹H NMR (400 MHz, d-CD₃OD, ppm): δ 7.83 (s, 1H), 7.43 (d, *J* = 8.9 Hz, 1H), 6.74 (dd, *J* = 8.9, 2.5 Hz, 1H), 6.53 (d, *J* = 2.4 Hz, 1H), 3.45-3.55 (m, 6H), 3.40-3.26 (m, 2H), 1.36-1.09 (m, 12H). ¹³C NMR (100 MHz, CDCl₃, ppm): δ 165.7, 159.3, 156.9, 151.3, 142.6, 129.5, 118.1, 109.2, 107.7, 97.1, 44.9, 43.3, 39.5, 14.2, 12.8, 12.4. ESI-HRMS (*m/z*, positive mode): calcd. 317.1865, observed 317.1853 for [M+H]⁺, calcd. 339.1685, observed 339.1681 for [M+Na]⁺.

Synthesis of compound 3. 7-chloro-*N,N*-dimethylbenzo[*c*][1,2,5]oxadiazole-4-sulfonamide (130 mg, 0.5 mmol), *N,N,N'*-tri(pyridin-2-ylmethyl)-ethane-1,2-diamine (162 mg, 0.5 mmol) and K₂CO₃ (69 mg, 0.5 mmol) were mixed in 10 mL of CH₃CN and refluxed for 24 h. After removing the solvent in vacuo, the residue was purified by silica gel column chromatography (petroleum ether/dichloromethane, 1:2, v/v) to yield compound **3** as a yellow powder (142 mg, 51%). ¹H NMR (400 MHz, CDCl₃, ppm): δ 8.55 (d, *J* = 4.5 Hz, 1H), 8.48 (d, *J* = 4.4 Hz, 2H), 7.68 (d, *J* = 8.3 Hz, 1H), 7.60 (m, 3H), 7.40 (d, *J* = 7.8 Hz, 2H), 7.18 (m, 1H), 7.12 (m, 3H), 5.98 (d, *J* = 8.3 Hz, 1H), 5.10 (s, 2H), 4.10 (m, 2H), 3.90 (s, 4H), 2.99 (t, *J* = 6.8 Hz, 2H), 2.84 (s, 6H). ¹³C NMR (100 MHz, CDCl₃, ppm): δ 158.8, 156.3, 149.9, 149.2, 147.1, 144.5, 141.9, 138.6, 137.0, 136.5, 123.2, 122.7, 122.3, 121.0, 108.6, 102.4, 60.9, 58.4, 51.6, 50.7, 37.9. ESI-HRMS (*m/z*, positive mode) calcd. 559.2240, observed: 559.2237 for [M+H]⁺, calcd. 581.2059, observed: 581.2056 for [M+Na]⁺.

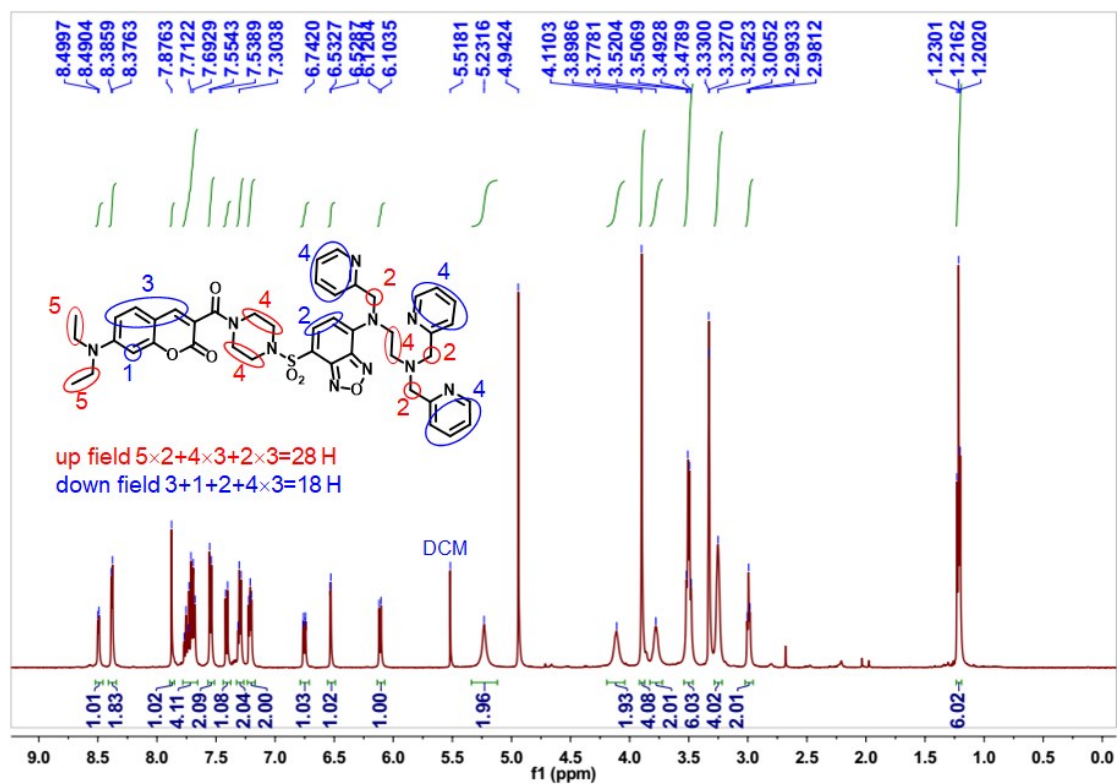


Fig. S1-1. ^1H NMR spectrum of CPBT in CD_3OD .

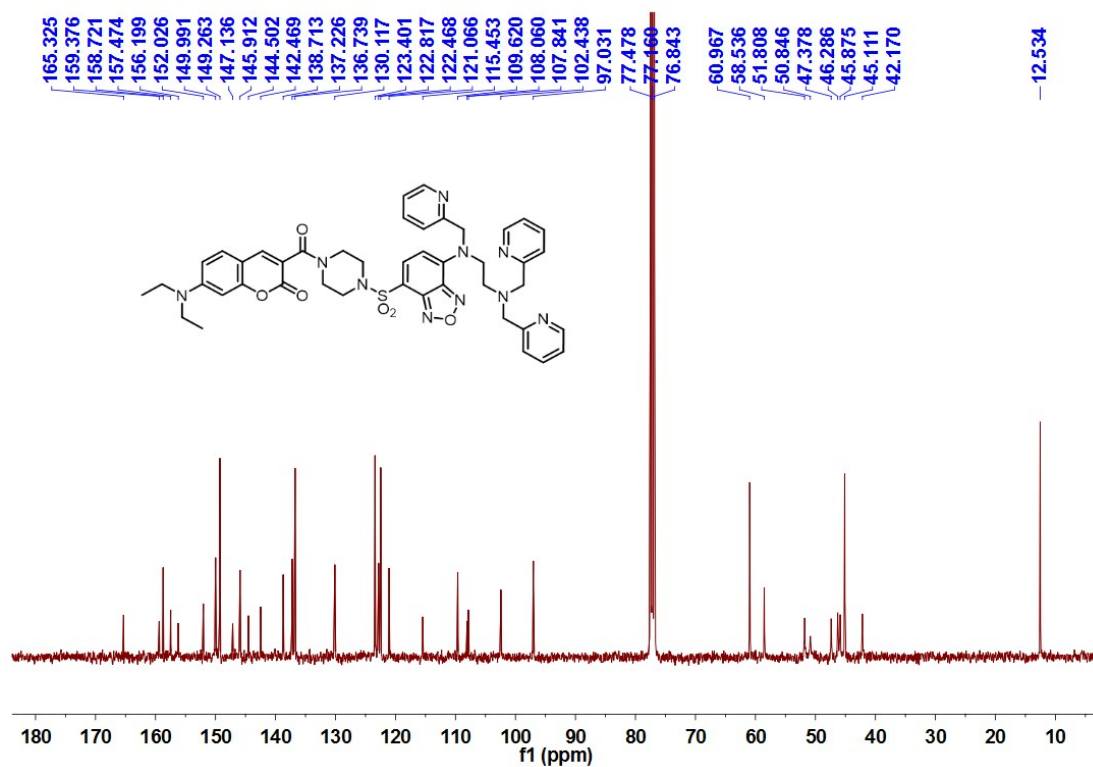


Fig. S1-2. ^{13}C NMR spectrum of CPBT in CDCl_3 .

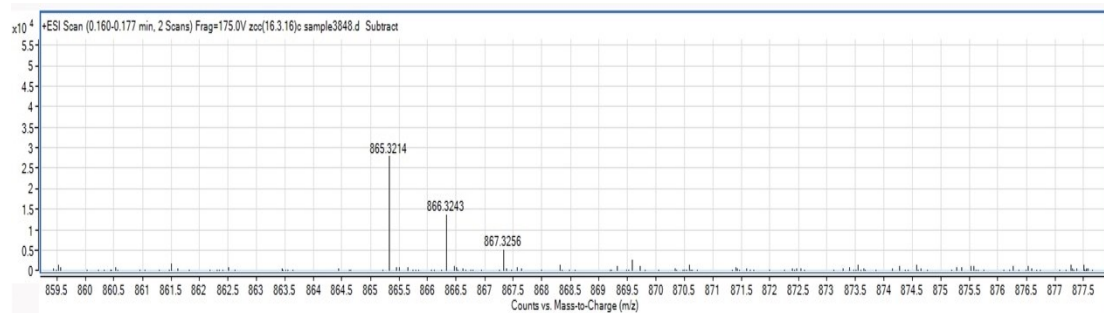


Fig. S1-3. ESI-HRMS of CPBT.

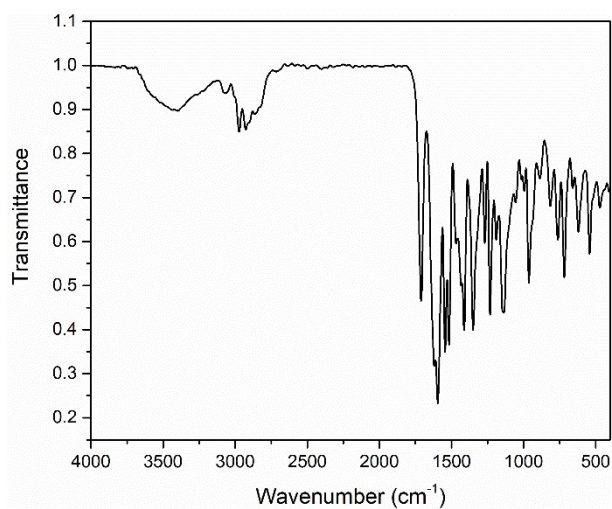


Fig. S1-4. FT-IR spectrum of CPBT.

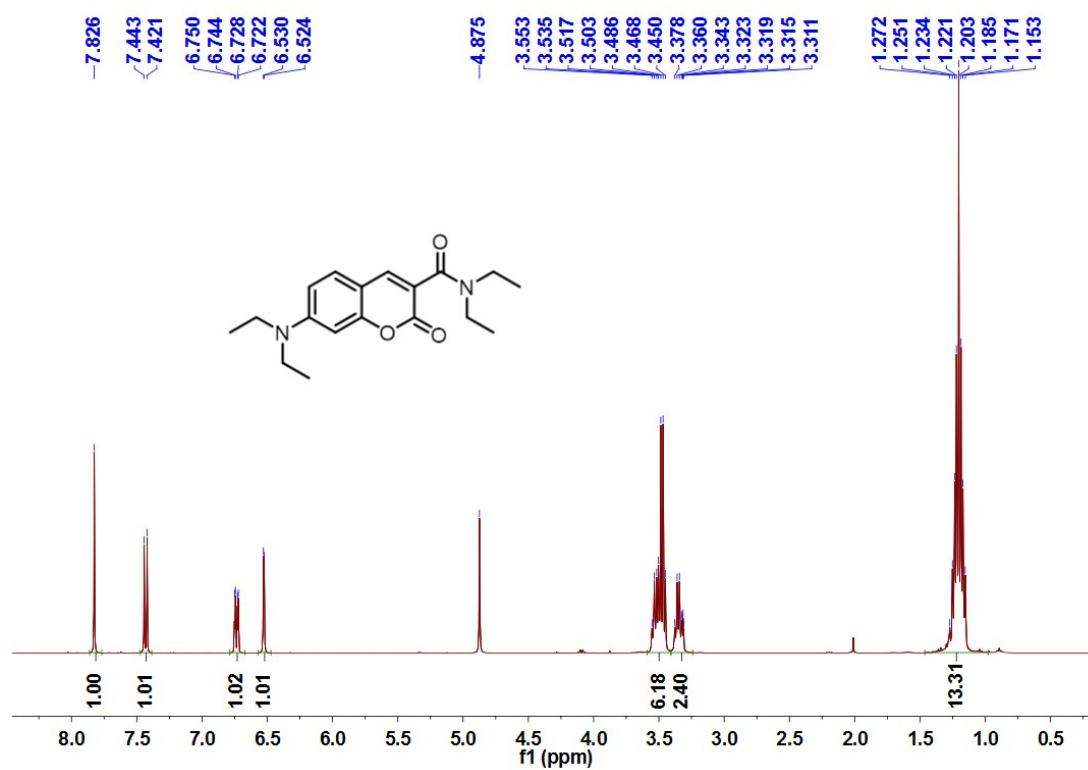


Fig. S2-1. ^1H NMR spectrum of compound 2 in CD_3OD .

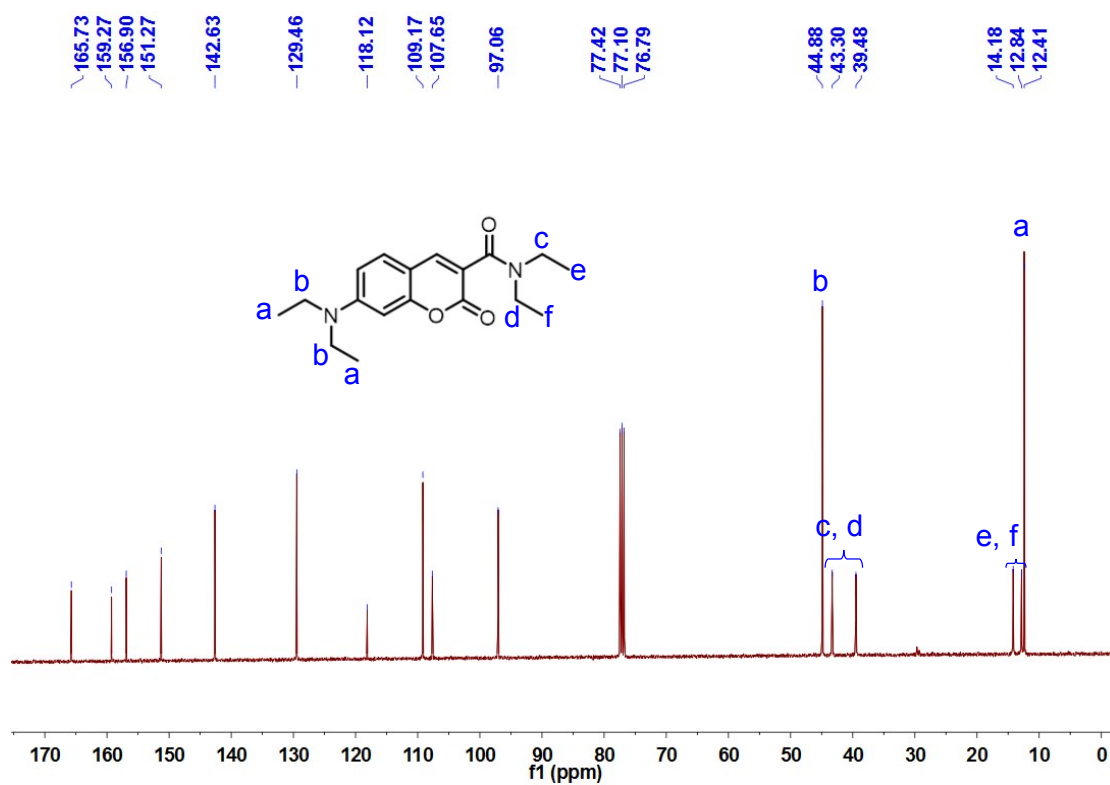


Fig. S2-2. ¹³C NMR spectrum of compound 2 in CDCl₃.

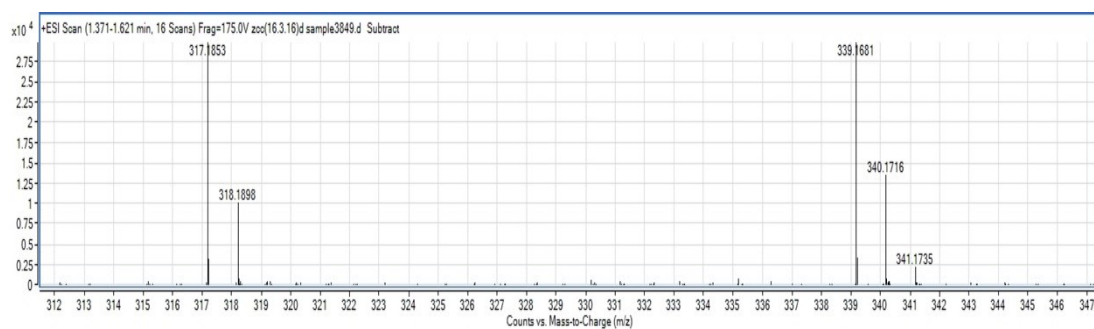


Fig. S2-3. ESI-HRMS of compound 2.

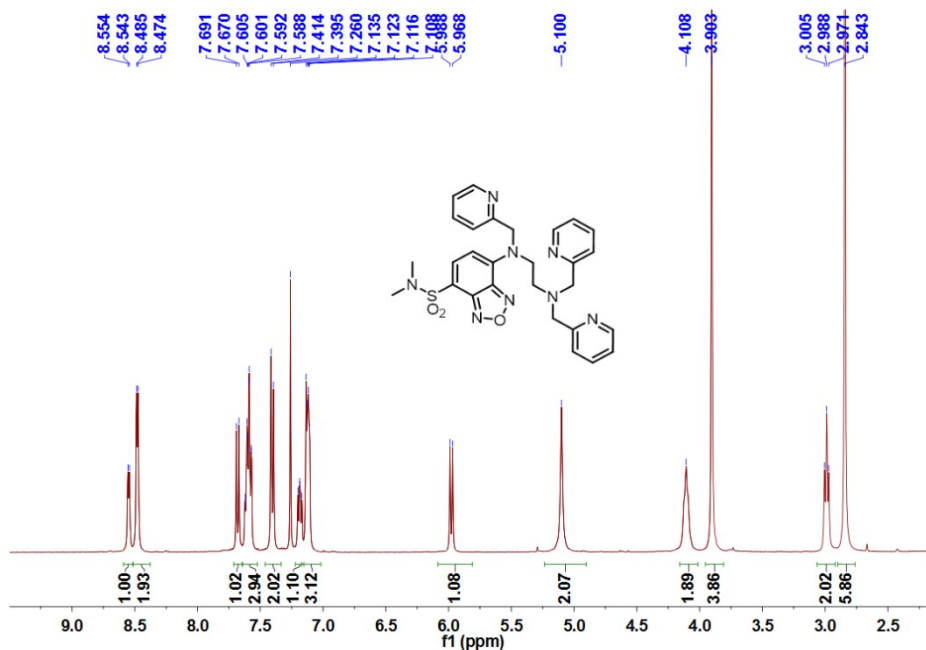


Fig. S3-1. ¹H NMR spectrum of compound 3 in CDCl₃.

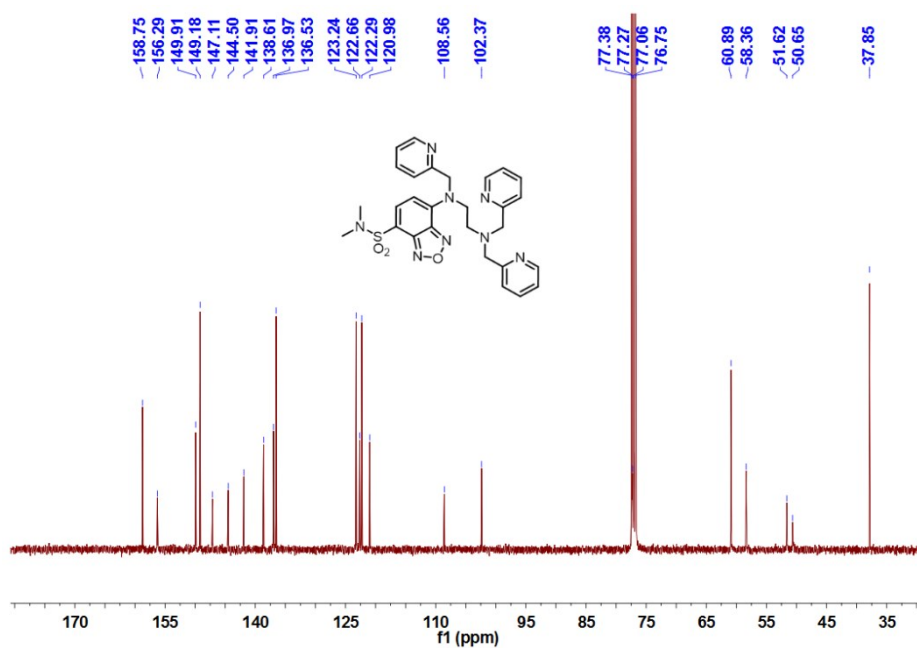


Fig. S3-2. ¹³C NMR spectrum of compound 3 in CDCl₃.

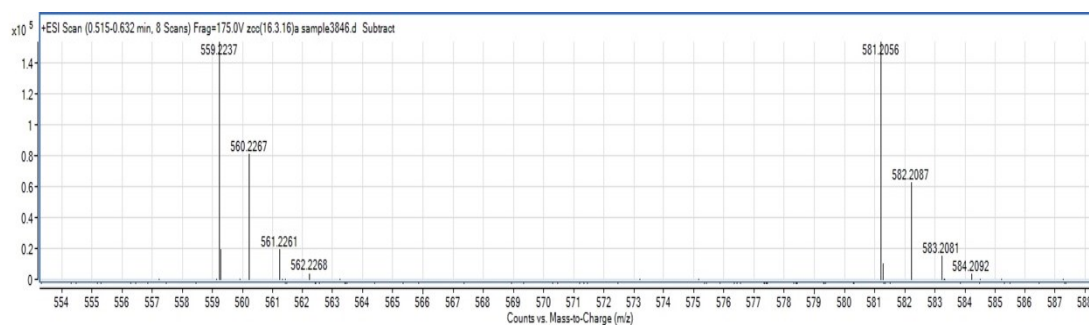


Fig. S3-3. ESI-HRMS of compound 3.

3. Spectroscopic studies.

All spectroscopic determinations were performed in HEPES buffer (50 mM HEPES, 100 mM KNO_3 , pH 7.4) containing 1% DMSO (v/v) unless indicated otherwise. The absorption and fluorescence spectra were obtained at concentrations of 10 and 5 μM , respectively, and the excitation wavelength for the fluorescence measurements was 415 nm. The fluorescence and UV-Vis absorption Zn^{2+} titration experiment was performed by titrating the sample with a $\text{Zn}(\text{NO}_3)_2$ solution in the range of 0-2.0 equivalents of sensor. The sensing selectivity of CPBT (5 μM) was analyzed in HEPES buffer (50 mM HEPES, 100 mM KNO_3 , pH 7.40, DMSO/ H_2O , 1/99) after adding 1 equivalent of Zn^{2+} , Cu^{2+} , Cd^{2+} , Co^{2+} , Cr^{3+} , Ni^{2+} , Fe^{2+} , Fe^{3+} , Mn^{2+} or Al^{3+} , or 1,000 equivalents of Na^+ , Ca^{2+} or Mg^{2+} . The detection limit for CPBT (5 μM) was obtained by determining the F_{480}/F_{560} ratio upon Zn^{2+} titration (0-1.5 μM) in the same buffer, and the detection limit (82 nM) was calculated as $3\sigma/\text{slope}$. The fluorescent pH-dependence of CPBT or CPBT- Zn^{2+} solution was confirmed by adjusting pH values with HCl or NaOH aqueous solutions. A series of buffered Zn^{2+} solutions were prepared for the determination of the dissociation constant of Zn^{2+} /CPBT complex.² Thus, various amounts of ZnNO_3 (0-20 mM) were added to the solution of HEPES buffer (HEPES 50 mM, pH 7.40, 100 mM KNO_3) containing 10 mM of ethylenebis(oxyethylenitrilo) tetraacetic acid (EGTA). For the determination of dissociation constant, the above mentioned buffered Zn^{2+} solutions were added with free sensor solution. The final concentration of total sensor in the mixture (containing 1% DMSO) is around 5 μM , and the emission spectra of the mixed solutions were determined respectively after complete mixing. The TPA cross-section of CPBT was calculated using a previously published equation based on the TPEF spectra of CPBT (5 μM in CH_3OH) upon excitation with a femtosecond pulsed laser (Coherent: pulse width ≤ 100 fs; 1000 Hz repetition rate) using rhodamine B as the reference.³

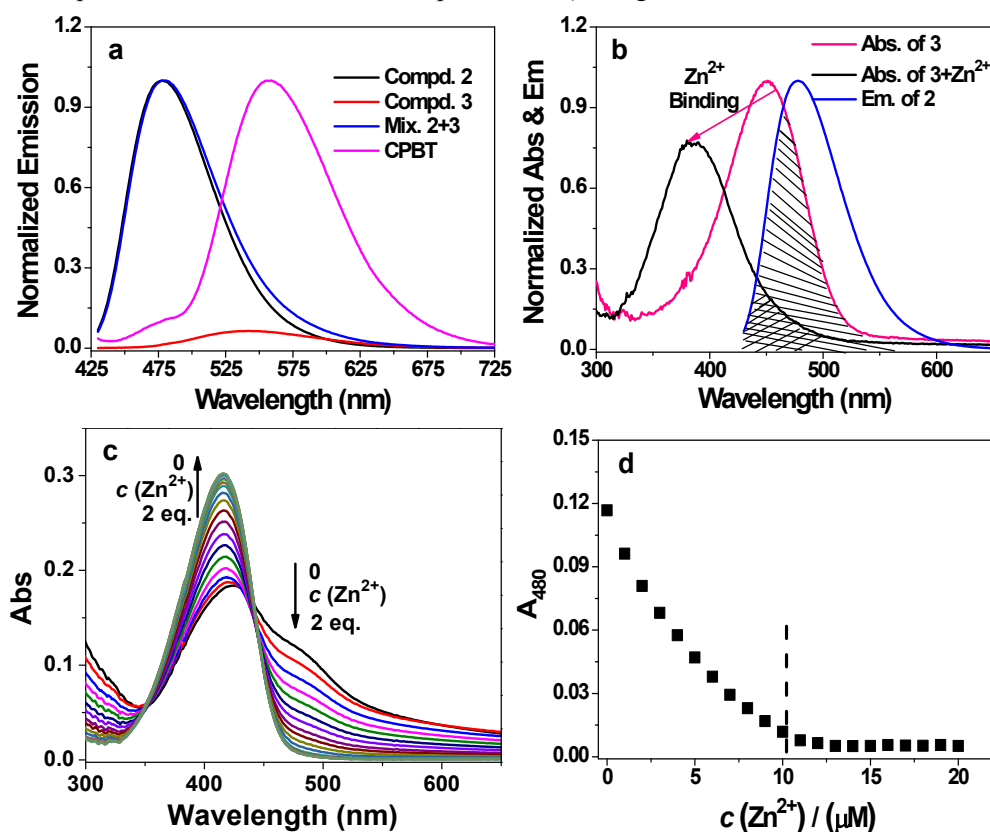


Fig. S4. (a) Normalized emission spectra of compounds **2**, **3**, CPBT, and the mixture of compounds **2** and **3** (1:1 molar ratio) in HEPES buffer (50 mM HEPES, 100 mM KNO₃, pH 7.40, DMSO/H₂O, 1/99). The concentrations of all compounds is 5 μM. λ_{ex} , 415 nm. (b) Normalized absorption/emission spectra of compounds **2** (5 μM) and **3** (5 μM) in the same buffer. The absorption spectrum of compound **3** in the presence of Zn²⁺ was obtained by adding 1 equivalent of Zn²⁺. (c) Absorption spectra of CPBT (10 μM) in the same buffer following Zn²⁺ titration (0-2.0 eq). (d) Zn²⁺ titration profile based on the absorbance at 480 nm.

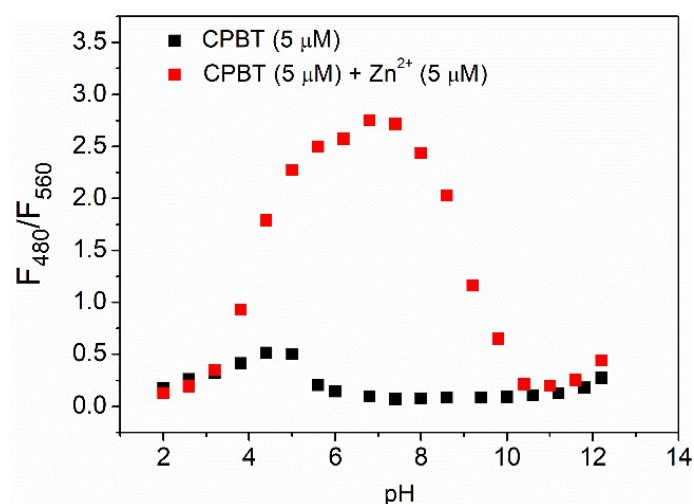


Fig. S5. The emission ratio F_{480}/F_{560} of CPBT and CPBT in the presence of 1 equivalent of Zn²⁺ at different pH.

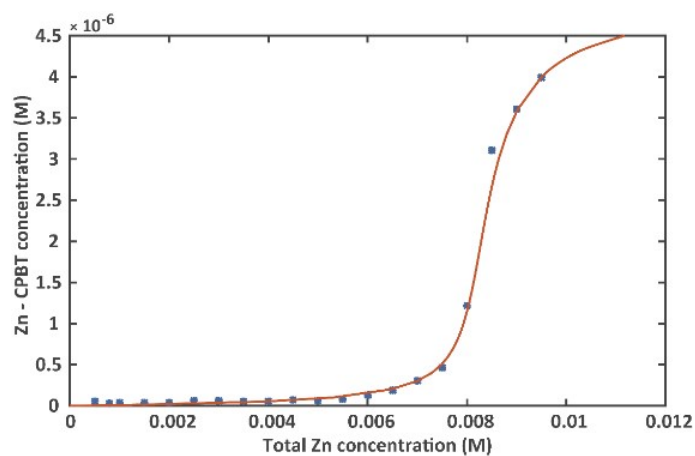


Fig. S6. Dissociation constant K_d titration curve of Zn²⁺-CPBT concentration as a function of total Zn²⁺ concentration.

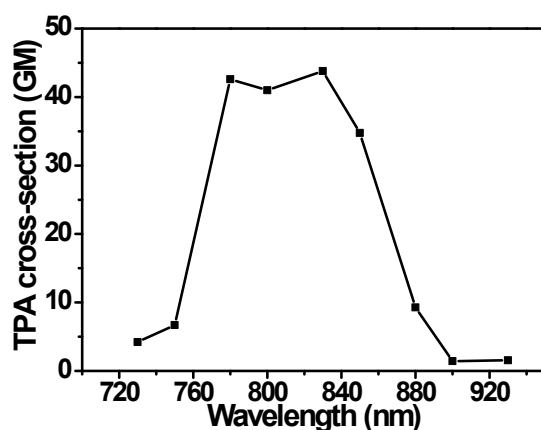


Fig. S7. Two-photon absorption cross-section of CPBT in the range of 730-930 nm. The two-photon excited fluorescence spectra of 10 μM CPBT in methanol were determined with a femtosecond pulsed laser (Coherent; pulse width ≤ 100 fs; 1000 Hz repetition rate; USA) with rhodamine B as the reference.

4. 2D ratiometric Zn^{2+} imaging

MCF-7 (DMEM), SKOV3 (RPMI 1640), A549 (RPMI 1640) and SGC7901 (RPMI 1640) cells were cultured in the indicated media supplemented with 10% fetal calf bovine serum (FBS) in an atmosphere of 5% CO_2 and 95% air at 37°C. All 2D ratiometric images were captured using a confocal laser scanning fluorescence microscope (Zeiss LSM710). For intracellular ratiometric imaging, cells were stained with CPBT (10 μM , 0.5 h) solution in PBS (1 \times) at ambient temperature. After rinsing with PBS, the cells were imaged in dual emission mode (green channel: 440-500 nm, red channel: 540-600 nm) upon excitation at 405 nm. After imaging, the cells were further incubated with ZnCl_2 :pyrithione (20 μM , 1:1, 0.5 h) solution followed by imaging in the same mode. The cells were then rinsed with PBS (3 times), incubated with TPEN (20 μM , 0.5 h), and imaged. The ratiometric images were based on the recorded green and red channel image pairs generated by the instrument using the default settings for ratiometric imaging. For imaging-based tracking of endogenous Zn^{2+} levels in cisplatin-treated MCF-7 and SKOV3 cells, the cells were stained with CPBT (10 μM , 1 h, 25°C) in PBS. After removing the CPBT solution, the cells were rinsed with PBS (3 times) followed by incubation with cisplatin (20 μM , 25°C) in PBS, after which ratiometric tracking was initiated by imaging every 0.5 h in dual emission mode. For 2D ratiometric Zn^{2+} imaging in zebrafish larvae, 3-day-old zebrafish larvae from Nanjing Eze-Rink, were incubated in tap water containing 0.0045% phenylthiourea (PTU) for 24 h post-fertilization at 28°C and were incubated with water containing CPBT (0.1 M) for 12 h. The larvae were then embedded in 1% carboxymethylcellulose, and the same dual emission mode was adopted using a 10 \times objective. The anterior and posterior parts of the larvae were imaged and the 2D ratiometric images of whole larvae were obtained by collaging the anterior and posterior images.

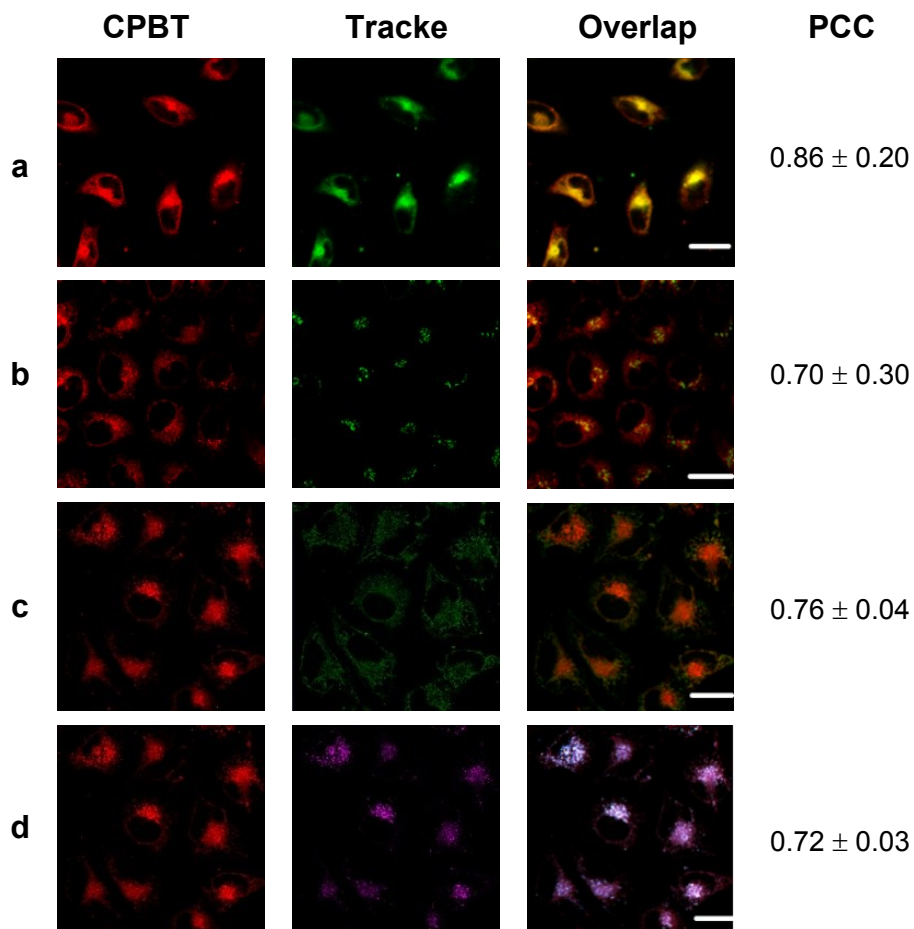


Fig. S8. Co-localization of CPBT with commercial endoplasmic reticulum (ER), Golgi apparatus, mitochondria and lysosome markers in MCF-7 cells *via* confocal fluorescence imaging. The cells were stained with 10 μ M CPBT for 30 min at room temperature followed by further staining with Mito-Tracker Deep Red 633 (1 μ M, 10 min), Lysosome-Tracker Red DND-99 (1 μ M, 10 min), ER-Tracker TM Red (1 μ M, 10 min), and Golgi-FITC (1 μ M, 10 min) respectively at room temperature. (a) images for ER-Tracker/CPBT co-localization; (b) images for Golgi-FITC /CPBT co-localization; (c) images for Mito-Tracker/CPBT co-localization; (d) images for Lysosome-Tracker/CPBT co-localization. Pearson's correlation coefficient (PCC) was calculated from the correlation plot of CPBT with ER-Tracker, Golgi-FITC, Mito-Tracker or Lysosome-Tracker. Scale bar, 20 μ m. Imaging conditions: CPBT imaging, λ_{ex} , 405 nm, band path, 440-500 nm; Mito-Tracker imaging, λ_{ex} , 633 nm, band path, 660-750 nm; ER tracker imaging, λ_{ex} , 543 nm, band path, 590-630 nm; Golgi tracker imaging, λ_{ex} , 488 nm, band path, 525-560 nm; lysosome tracker imaging, λ_{ex} , 543 nm, band path, 570-600 nm.

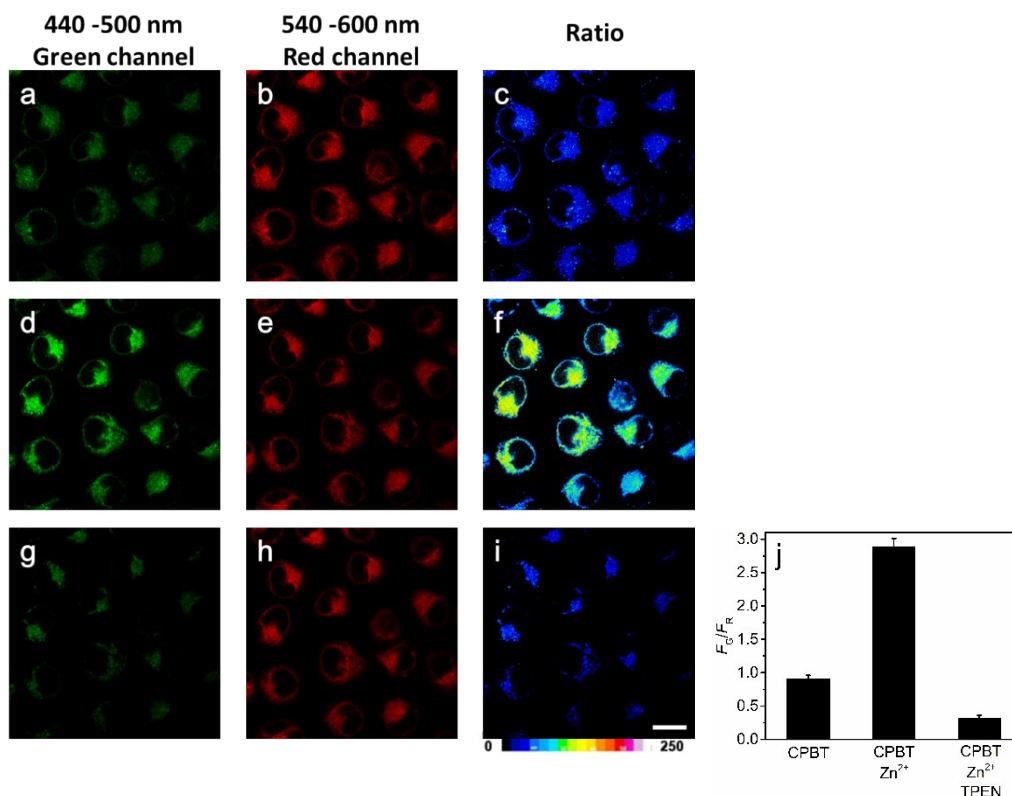


Fig. S9. Confocal fluorescence imaging of MCF-7 cells stained by CPBT (10 μ M, 30 min) *via* a dual channel mode upon excitation at 405 nm. Green channel, 440-500 nm; red channel, 540-600 nm; ratio channel was generated from the green channel divided by the red channel. All incubation and imaging procedures were carried out at 25°C. (a-c) Images of the CPBT-stained MCF-7 cells; (d-f) images for the stained cells in (a) treated further with Zn^{2+} incubation (20 μ M $ZnCl_2$ /pyrithione, 1:1, 30 min); (g-i) images of the cells in (d) incubated further with 20 μ M TPEN for 30 min; (j) histogram of ratio values averaged from 5 randomly selected fields of ratio channel cells in (c), (f) and (i), data are shown as mean \pm SD ($n = 5$). Scale bar, 20 μ m; color strip, ratio bar.

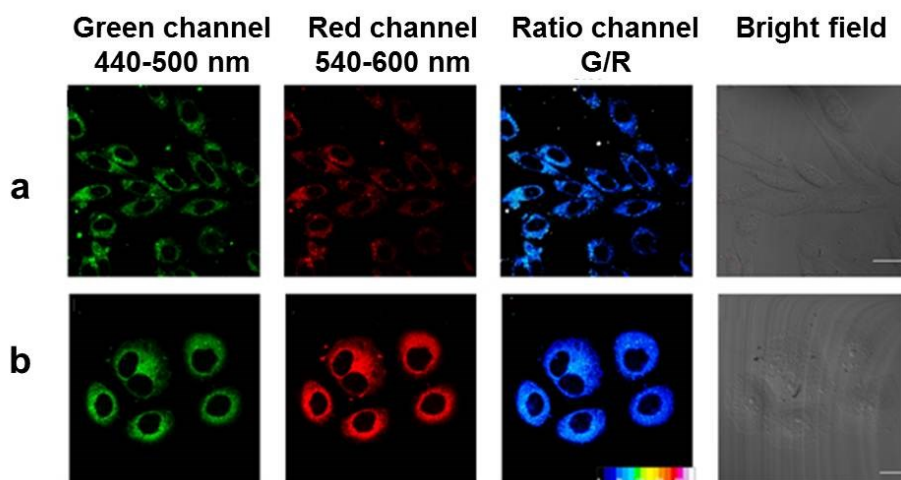


Fig. S10. Fluorescence ratiometric imaging of A549 (a) and SGC7901 (b) cells stained by CPBT (10 μ M, 30 min, 25°C) with a dual emission mode upon excitation at 405 nm. Green channel, 440-500 nm; red channel, 540-600 nm; ratio channel was generated from the green channel divided by the red

channel. Scar bar, 20 μm .

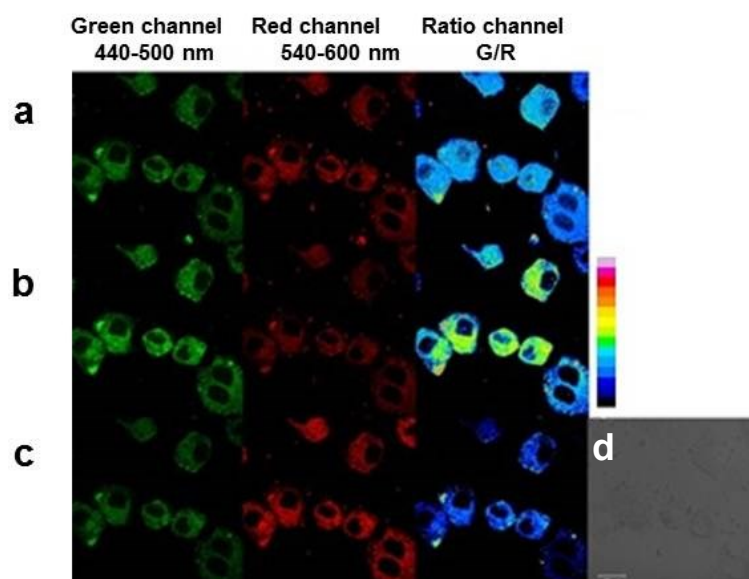


Fig. S11. Fluorescence ratiometric Zn^{2+} imaging in the CPBT-stained (10 μM , 30 min) SKOV3 cells *via* a dual channel mode (green channel, 440-500 nm; red channel, 540-600 nm) upon excitation at 405 nm. All incubation and imaging procedures were carried out at 25 $^{\circ}\text{C}$. (a) Images of the CPBT-stained SKOV3 cells; (b) images of the cells in (a) after further incubation with 20 μM Zn^{2+} /pyrithione (1:1) solution for 30 min; (c) images of the cells in (b) after incubation with 20 μM TPEN for 30 min; (d) bright field image. Scale bar, 20 μm ; color strip, ratio bar.

5. 3D ratiometric Zn^{2+} imaging

The stained larvae (see 2D imaging) were embedded in methyl cellulose and each plane was imaged in the Z-stack mode using a Zeiss LSM710 microscope with the same dual emission mode used for 2D imaging; the stack interval was 1 μm . The ratiometric image of each stack was automatically generated from the recorded green channel image divided by the red channel image for the same stack by the instrument. The 3D reconstructed images for the red and green channels and ratiometric images were generated using the ZEN 2009 light edition program.

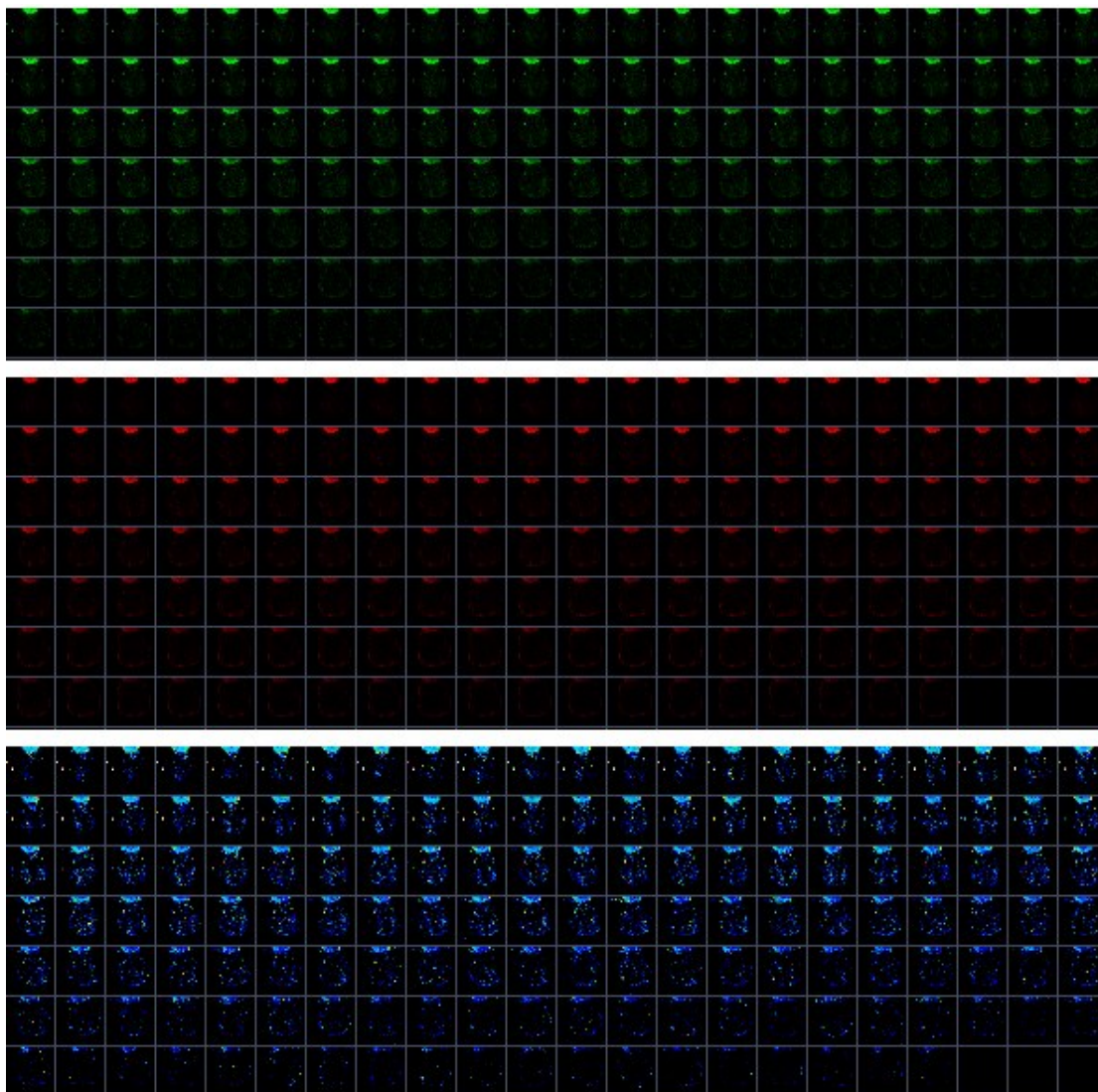


Fig. S12. Ratiometric fluorescence imaging for endogenous labile Zn^{2+} in the head of a 3-day-old zebra fish larva stained by CPBT (0.1 μ M, 12 h, 28°C) with a Z-stack mode, and stack interval is 1 μ m. At each imaging depth, a dual emission mode with a green channel of 440-500 nm and a red channel of 540-600 nm were adopted for imaging. The effective imaging depth attains to 150 μ m. λ_{ex} , 405 nm. Upper row, the green channel images at different imaging depth; middle row, the red channel images at different imaging depth; lower row, the ratiometric images at different imaging depth.

6. Cisplatin-induced Zn^{2+} change monitoring.

Cells were seeded in 35-mm dishes at a density of 10^4 cells/mL and cultured with DMEM (MCF-7 cells) or RPMI 1640 (SKOV3 cells) supplemented with 10% FBS in an atmosphere of 5% CO_2 and 95% air at 37°C until the cells reached 80% confluence. The cells were then digested with trypsin followed by rinses with PBS (1 \times , 3 times). The cells were stained with CPBT (10 μ M, 1 h) in PBS at 0°C. After removing the staining medium, the cells were rinsed with PBS three times and resuspended in PBS. Three aliquots of this suspension were treated with PBS, $ZnCl_2$ /pyrithione (20 μ M, 1:1) and then TPEN (20 μ M) for 0.5 h at 0°C to confirm the effectiveness of the ratiometric flow cytometry assay for Zn^{2+} . The cells were analyzed with a

flow cytometer (BD LSR Fortessa™) in dual emission mode (green channel: filter 450 ± 25 nm, red channel: filter 570 ± 15 nm, λ_{ex} 405 nm).

For the ratiometric flow cytometry assay of tracking labile Zn^{2+} levels change in cisplatin-treated cells, the CPBT stained cells were cultured with culture medium containing $20 \mu M$ cisplatin ($37^\circ C$) for 0, 2, 4, 6, 8, 10 and 12 h. The cells were then detached with trypsin followed by a rinse with PBS ($1\times$, 3 times). Cisplatin-induced fluctuations in labile Zn^{2+} levels were measured at $25^\circ C$ in PBS containing cisplatin to avoid interference from the culture medium. The scarcity of nutrients may alter the cellular response to cisplatin, therefore, the ratiometric Zn^{2+} flow cytometric assay was also used to track the Zn^{2+} fluctuations in batches of cells following the addition of cisplatin ($20 \mu M$, $37^\circ C$) to the culture medium. Since the ratiometric flow cytometry assay does not depend on the intracellular sensor concentration, the temporal tracking of Zn^{2+} levels was achieved by determining the β angles of different batches of cells with different cisplatin incubation times. Cells with different cisplatin incubation time were stained with the CPBT solution ($10 \mu M$, 1 h, at $0^\circ C$) after dissociation and a PBS rinse.

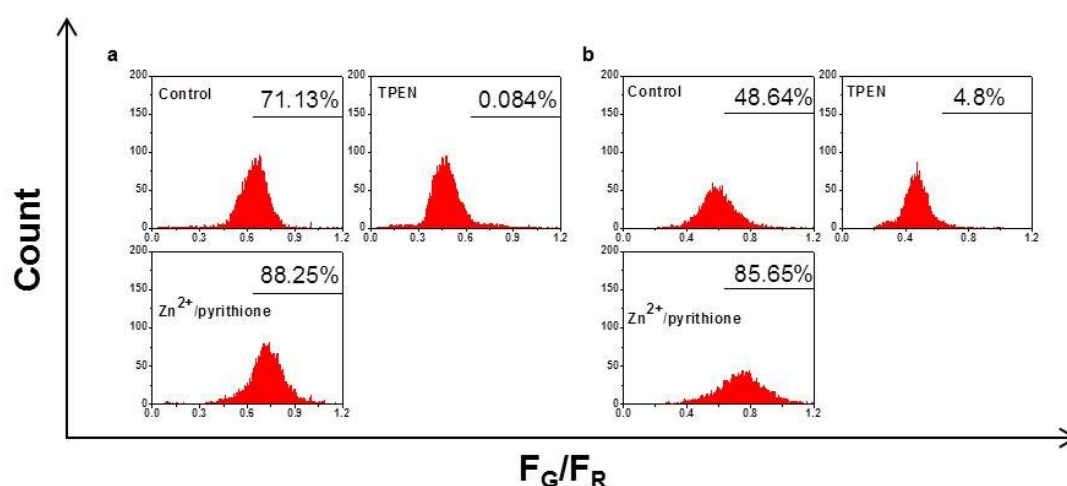


Fig. S13. Cell distribution pattern of SKOV3 (a) and MCF-7 (b) cells determined in the dual channel ratiometric flow cytometric assay for intracellular endogenous labile Zn^{2+} according to the average F_G/F_R ratio (fluorescence ratio of green channel to red channel). Green channel, 450 ± 25 nm; red channel, 570 ± 15 nm. λ_{ex} , 405 nm. $n \geq 3$, $p \leq 0.05$, cell number = 10000. The dissociated cells were stained with CPBT ($10 \mu M$, 1 h) upon being cooled by ice, followed by rinse with PBS ($1\times$). Then the cells were divided into three batches, which was treated further with $20 \mu M$ TPEN (30 min), Zn^{2+} /pyrithione ($20 \mu M$, 1:1, 30 min), or PBS ($1\times$, 30 min control) for the ratiometric flow cytometric assay. The percentages indicate the proportion of cells with F_G/F_R higher than 0.6.

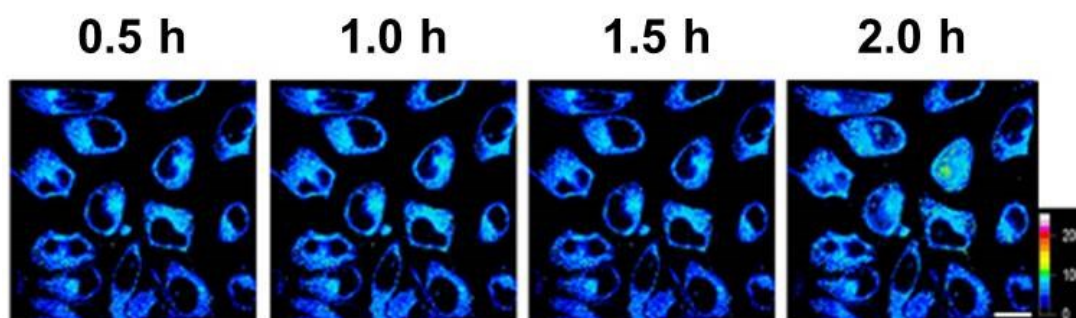


Fig. S14. Ratiometric images of the CPBT-stained ($10 \mu M$, 60 min) MCF-7 cells upon incubation with

PBS (1×) for 0.5, 1, 1.5 and 2 h. A dual channel mode (green channel, 440-500 nm; red channel, 540-600 nm) upon excitation at 405 nm was adopted. All staining, incubation and imaging procedures were carried out at 25°C. Scale bar, 10 μ m.

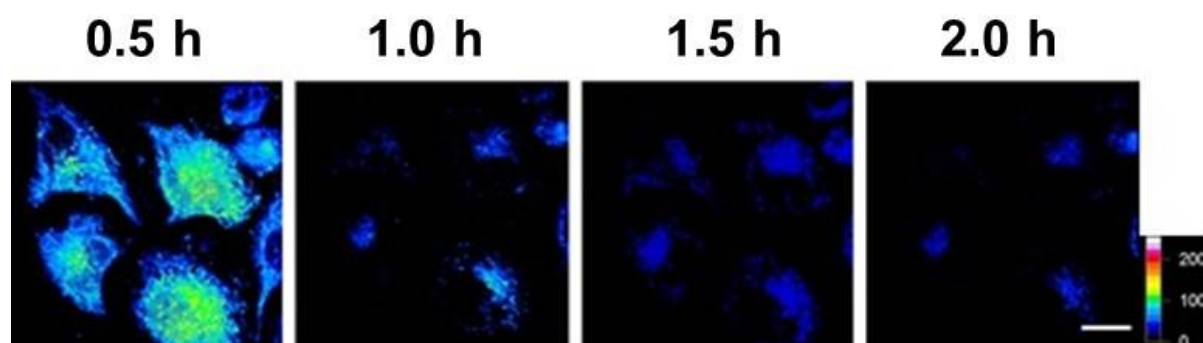


Fig. S15. Ratio images of the CPBT-stained (10 μ M, 60 min) MCF-7 cells incubated further with 20 μ M cisplatin for 0.5, 1, 1.5 and 2 h. A dual channel mode (green channel, 440-500 nm; red channel, 540-600 nm) upon excitation at 405 nm was adopted. All staining, incubation and imaging procedures were carried out at 25°C. Scale bar, 10 μ m.

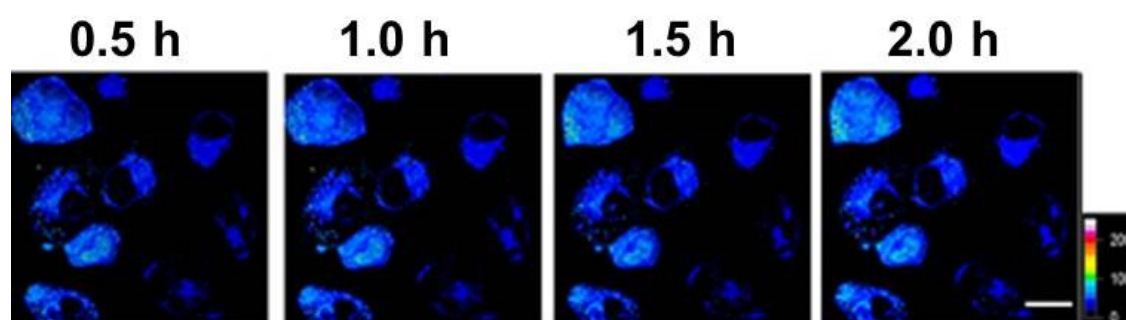


Fig. S16. Ratiometric images of the CPBT-stained (10 μ M, 60 min) SKOV3 cells upon incubation with PBS (1×) for 0.5, 1, 1.5 and 2 h. A dual channel mode (green channel, 440-500 nm; red channel, 540-600 nm) upon excitation at 405 nm was adopted. All staining, incubation and imaging procedures were carried out at 25°C. Scale bar, 10 μ m.

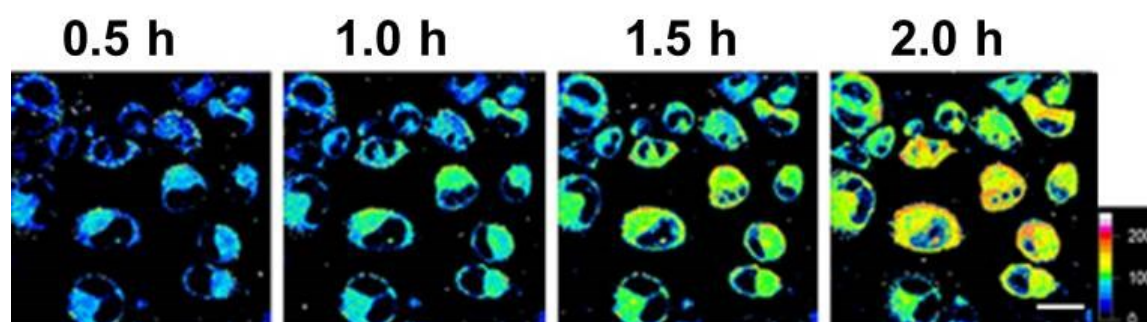


Fig. S17. Ratio images of the CPBT-stained (10 μ M, 60 min) SKOV3 cells incubated with 20 μ M cisplatin for 0.5, 1, 1.5 and 2 h. A dual channel mode (green channel, 440-500 nm; red channel, 540-600 nm) upon excitation at 405 nm was adopted. All staining, incubation and imaging procedures were

carried out at 25°C. Scale bar, 10 μm .

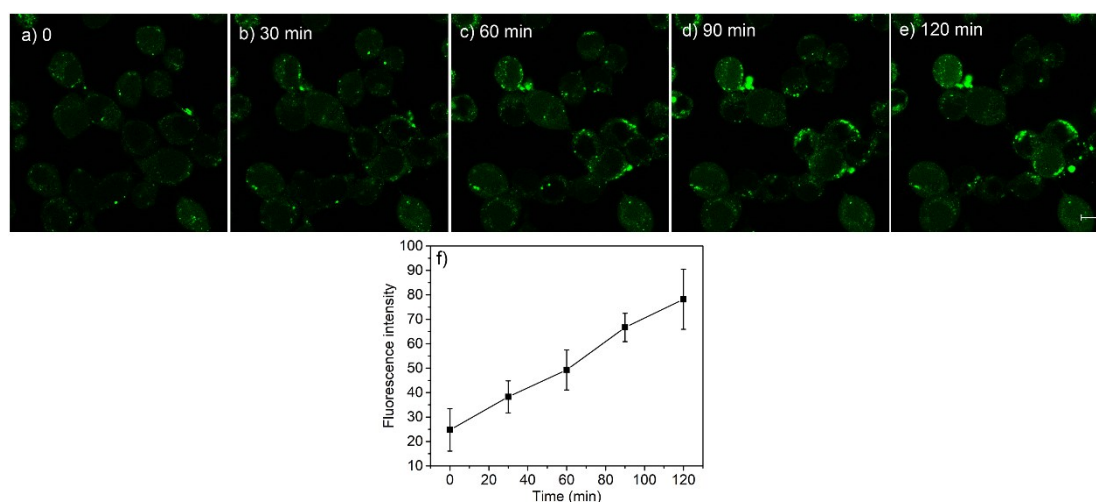


Fig. S18. (a-e) Fluorescence images of FluoZin-3 (2 μM , 1 h, 25 $^{\circ}\text{C}$) stained SKOV-3 cells incubated with cisplatin (20 μM , 25 $^{\circ}\text{C}$) at 0 min (a), 30 min (b), 60 min (c), 90 min (d) and 120 min (e). (f) The temporal profile of average intracellular emission fluorescence intensity. λ_{ex} , 488 nm; λ_{em} , 503-572 nm. Scale bar, 10 μm .

FluoZin-3 stained SKOV-3 cells showed a gradual fluorescence increase response to increased endogenous zinc level stimulated by cisplatin, similar to the results obtained using CPBT.

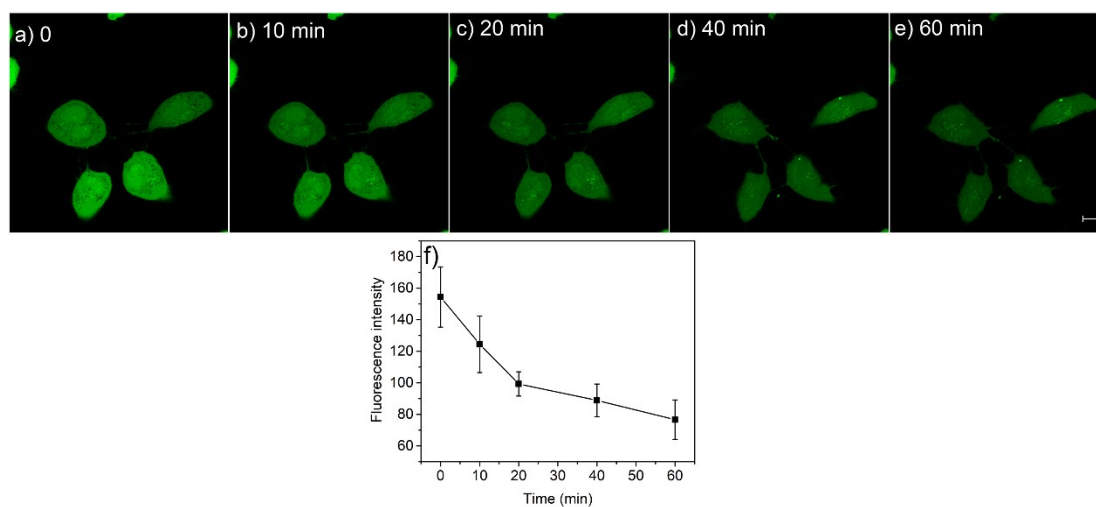


Fig. S19. (a-e) Fluorescence images of FluoZin-3 (2 μM , 1 h, 25 $^{\circ}\text{C}$) stained MCF-7 cells incubated with cisplatin (20 μM , 25 $^{\circ}\text{C}$) at 0 min (a), 10 min (b), 20 min (c), 40 min (d) and 60 min (e). (f) The temporal profile of average intracellular emission fluorescence intensity. λ_{ex} , 488 nm; λ_{em} , 503-572 nm. Scale bar, 10 μm .

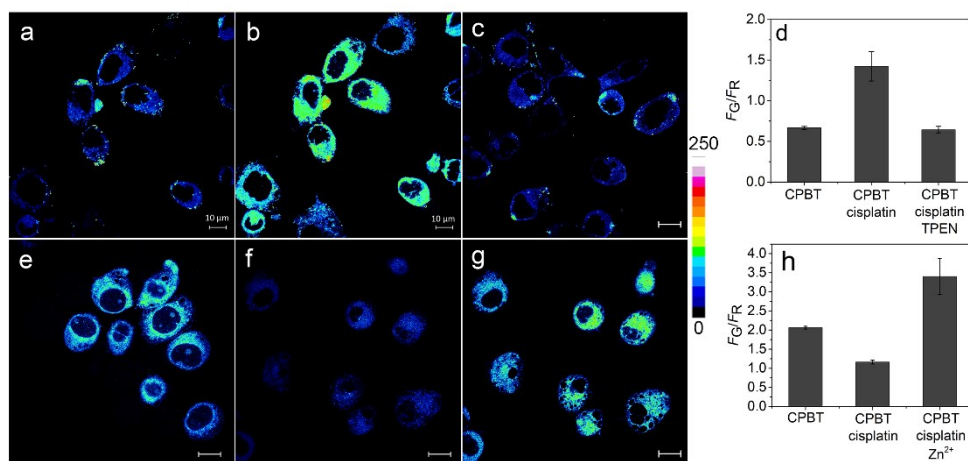


Fig. S20. (a-c, e-g) Ratiometric fluorescence images of SKOV3 (a-c) and MCF-7 (e-g) cells stained with CPBT (10 μM , 1 h, 25 $^{\circ}\text{C}$) in the absence (a, e) and presence (b, f) of cisplatin (20 μM , 1 h, 25 $^{\circ}\text{C}$); cells co-incubated with cisplatin (20 μM , 1 h, 25 $^{\circ}\text{C}$) and TPEN (20 μM , 1 h, 25 $^{\circ}\text{C}$) (c); and cells in (f) incubated further with 20 μM Zn^{2+} ($\text{ZnCl}_2/\text{pyrithione}$, 1:1) for 30 min (g). (d, h) The histogram profiles (d, SKOV3 cells; h, MCF-7 cells) of average intracellular emission ratio (F_G/F_R) of green channel (F_G , wavelength 440-500 nm) to red channel (F_R , wavelength 540-600 nm) intensity. Ratiometric fluorescence images were generated from the ratio of green channel to red channel. λ_{ex} , 405 nm; scale bar, 10 μm .

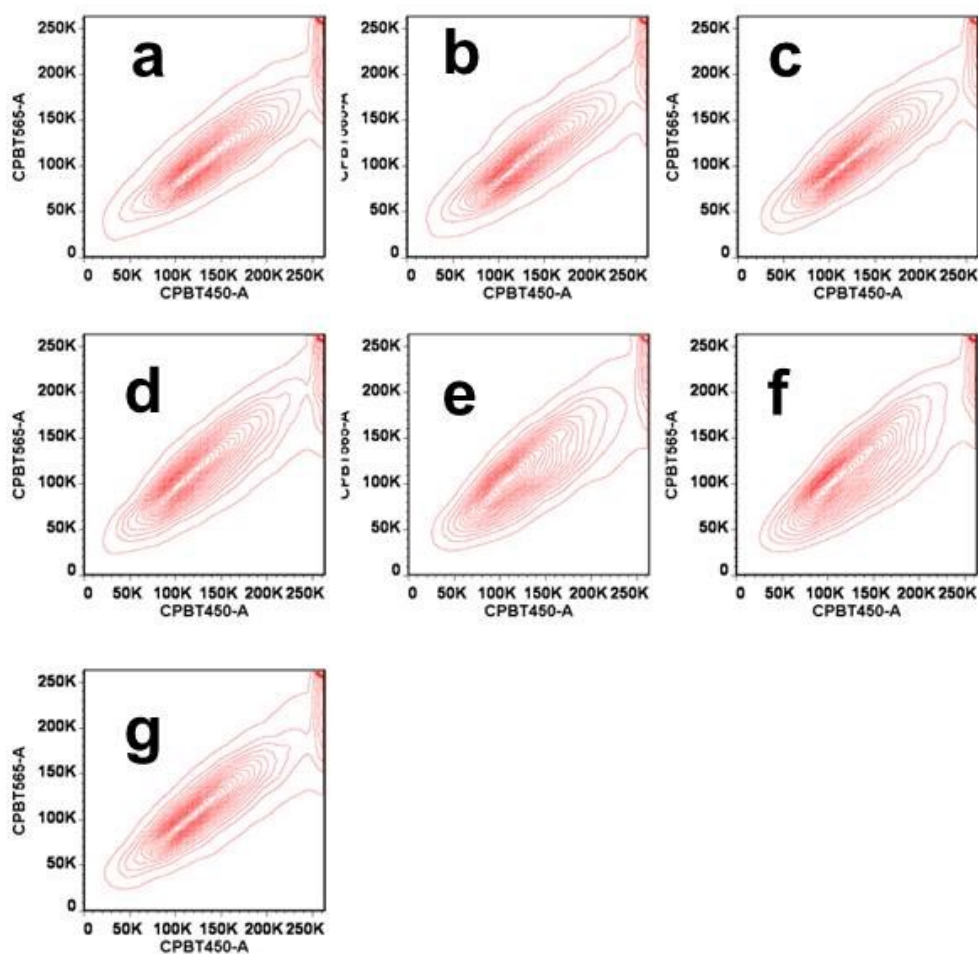


Fig. S21. Cell population contour plots (F_G - F_R coordinates) determined in the ratiometric flow cytometric assay for endogenous labile Zn^{2+} in MCF-7 cells incubated with cisplatin (20 μ M, 37°C) in the presence of culture medium. Cells were cultured in dishes (35 mm) till the adherent rate attains to 80%. At the desired cisplatin incubation time, the cells were digested with trypsin followed by rinse with PBS for 3 times, then the cells were stained with 10 μ M CPBT for 1 h upon being cooled by ice. After that, the cells were rinsed with PBS for dual channel flow cytometric determination. Green channel, 450 \pm 25 nm; red channel, 570 \pm 15 nm. $n \geq 3$, $p \leq 0.05$, cell number = 10000. The β angles for the cells of 0 h (a), 2 h (b), 4 h (c), 6 h (d), 8 h (e), 10 h (f), 12 h (g) of cisplatin incubation were 52.1 \pm 0.1°, 50.4 \pm 0.2°, 49.4 \pm 0.2°, 46.6 \pm 0.2°, 46.0 \pm 0.2°, 46.2 \pm 0.1°, 49.1 \pm 0.1°, respectively.

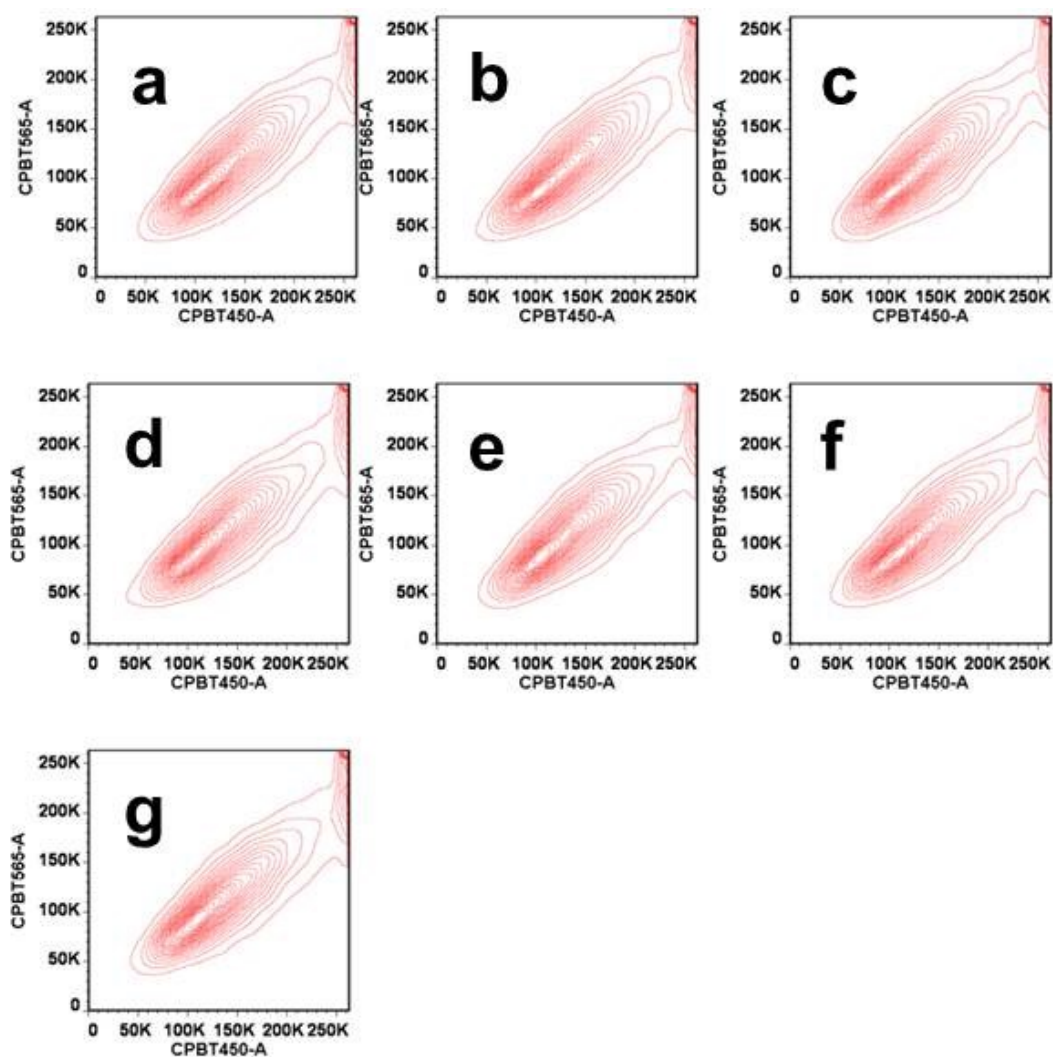


Fig. S22. Cell population contour plots (F_G - F_R coordinates) determined in the ratiometric flow cytometric assay for endogenous labile Zn^{2+} in MCF-7 cells incubated with PBS in the presence of culture medium (37°C). Cells were cultured in dishes (35 mm) till the adherent rate attains to 80%. At the desired incubation time, the cells were digested with trypsin followed by rinse with PBS for 3 times, then the cells were stained with 10 μ M CPBT for 1 h upon being cooled by ice. After that, the cells were rinsed with PBS for dual channel flow cytometric determination. Green channel, 450 \pm 25 nm; red channel, 570 \pm 15 nm. $n \geq 3$, $p \leq 0.05$, cell number = 10000. The β angles for the cells of 0 h (a), 2

h (b), 4 h (c), 6 h (d), 8 h (e), 10 h (f), 12 h (g) of PBS incubation were $49.5 \pm 0.1^\circ$, $50.0 \pm 0.1^\circ$, $49.9 \pm 0.2^\circ$, $49.8 \pm 0.1^\circ$, $49.8 \pm 0.2^\circ$, $49.6 \pm 0.1^\circ$, and $50.0 \pm 0.2^\circ$, respectively.

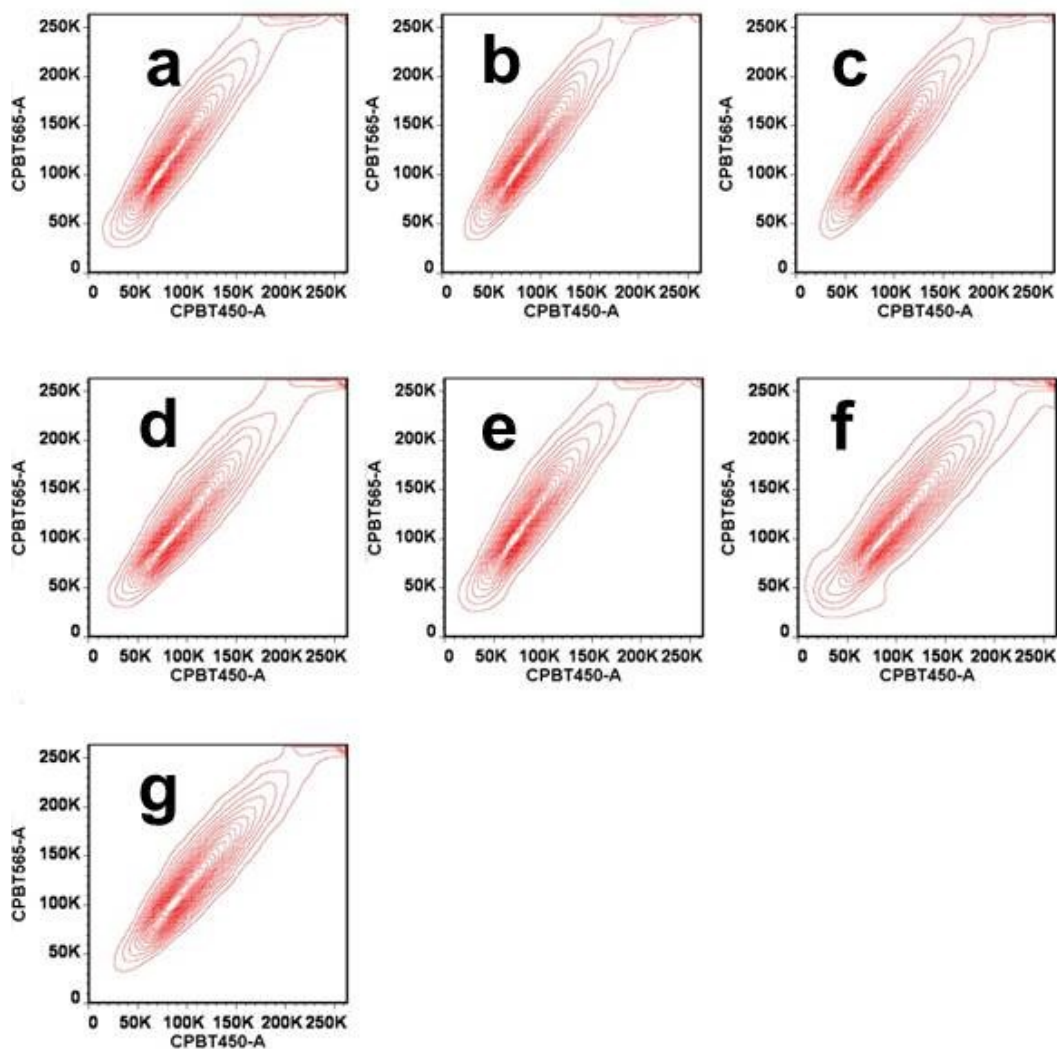


Fig. S23. Cell population contour plots (F_G - F_R coordinates) determined in the ratiometric flow cytometric assay for endogenous labile Zn^{2+} in SKOV3 cells incubated with cisplatin ($20 \mu M$, $37^\circ C$) in the presence of culture medium. Cells were cultured in dishes (35 mm) till the adherent rate attains to 80%. At the desired cisplatin incubation time, the cells were digested with trypsin followed by rinse with PBS for 3 times, then the cells were stained with $10 \mu M$ CPBT for 1 h upon being cooled by ice. After that, the cells were rinsed with PBS for dual channel flow cytometric determination. Green channel, 450 ± 25 nm; red channel, 570 ± 15 nm. $n \geq 3$, $p \leq 0.05$, cell number = 10000. The β angles for the cells of 0 (a), 2h (b), 4h (c), 6h (d), 8h (e), 10h (f), 12h (g) of cisplatin incubation were $35.6 \pm 0.2^\circ$, $36.0 \pm 0.2^\circ$, $36.6 \pm 0.2^\circ$, $39.8 \pm 0.1^\circ$, $40.2 \pm 0.2^\circ$, $40.6 \pm 0.3^\circ$, $40.7 \pm 0.3^\circ$, respectively.

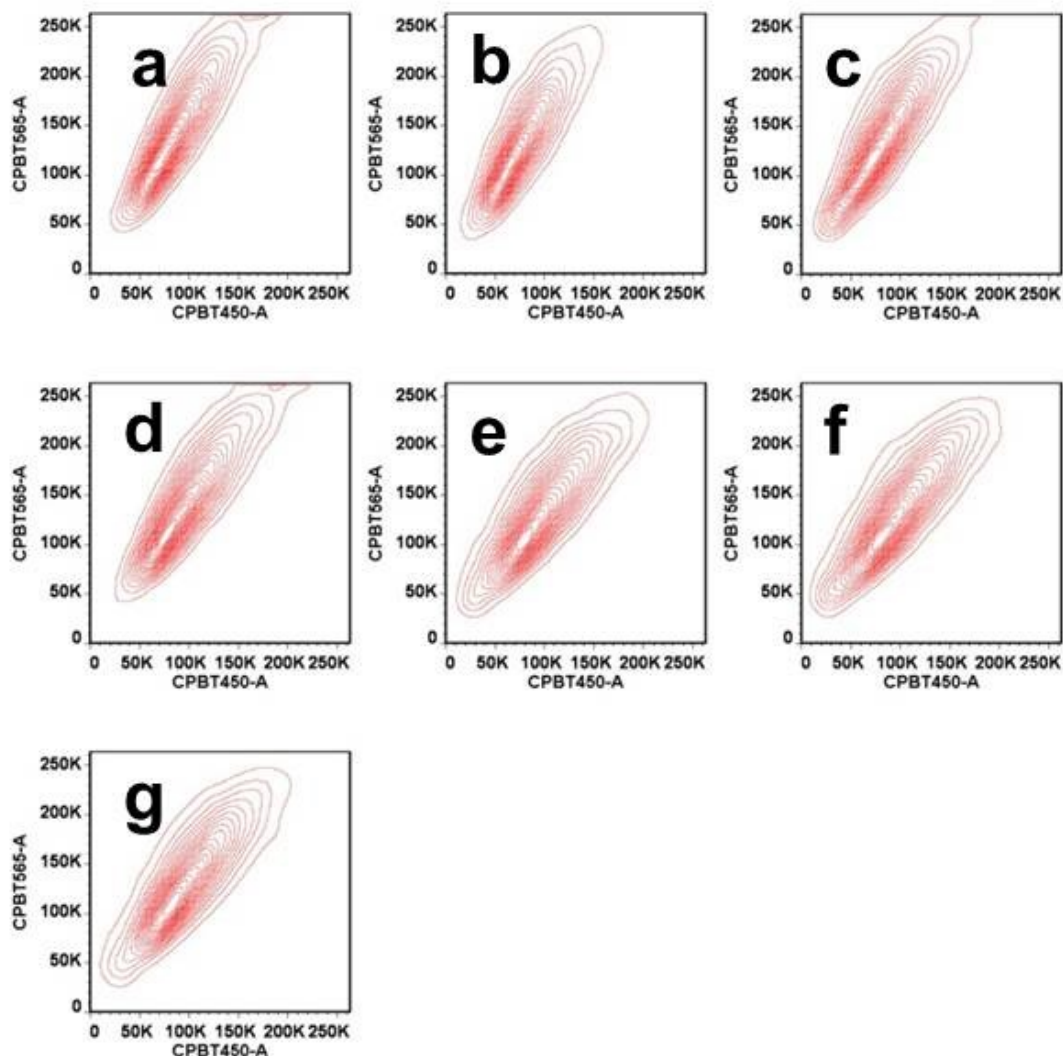


Fig. S24. Cell population contour plots (F_G - F_R coordinates) determined in the ratiometric flow cytometric assay for endogenous labile Zn^{2+} in SKOV3 cells incubated with PBS in the presence of culture medium ($37^\circ C$). Cells were cultured in dishes (35 mm) till the adherent rate attains to 80%. At the desired incubation time, the cells were digested with trypsin followed by rinse with PBS for 3 times, then the cells were stained with $10 \mu M$ CPBT for 1 h upon being cooled by ice. After that, the cells were rinsed with PBS for dual channel flow cytometric determination. Green channel, 450 ± 25 nm; red channel, 570 ± 15 nm. $n \geq 3$, $p < 0.05$, cell number = 10000. The β angles for the cells of 0 h (a), 2 h (b), 4 h (c), 6 h (d), 8 h (e), 10 h (f), 12 h (g) of PBS incubation were $29.9 \pm 0.1^\circ$, $29.6 \pm 0.2^\circ$, $31.1 \pm 0.1^\circ$, $30.2 \pm 0.1^\circ$, $31.5 \pm 0.2^\circ$, $31.5 \pm 0.1^\circ$, $31.6 \pm 0.2^\circ$, respectively.

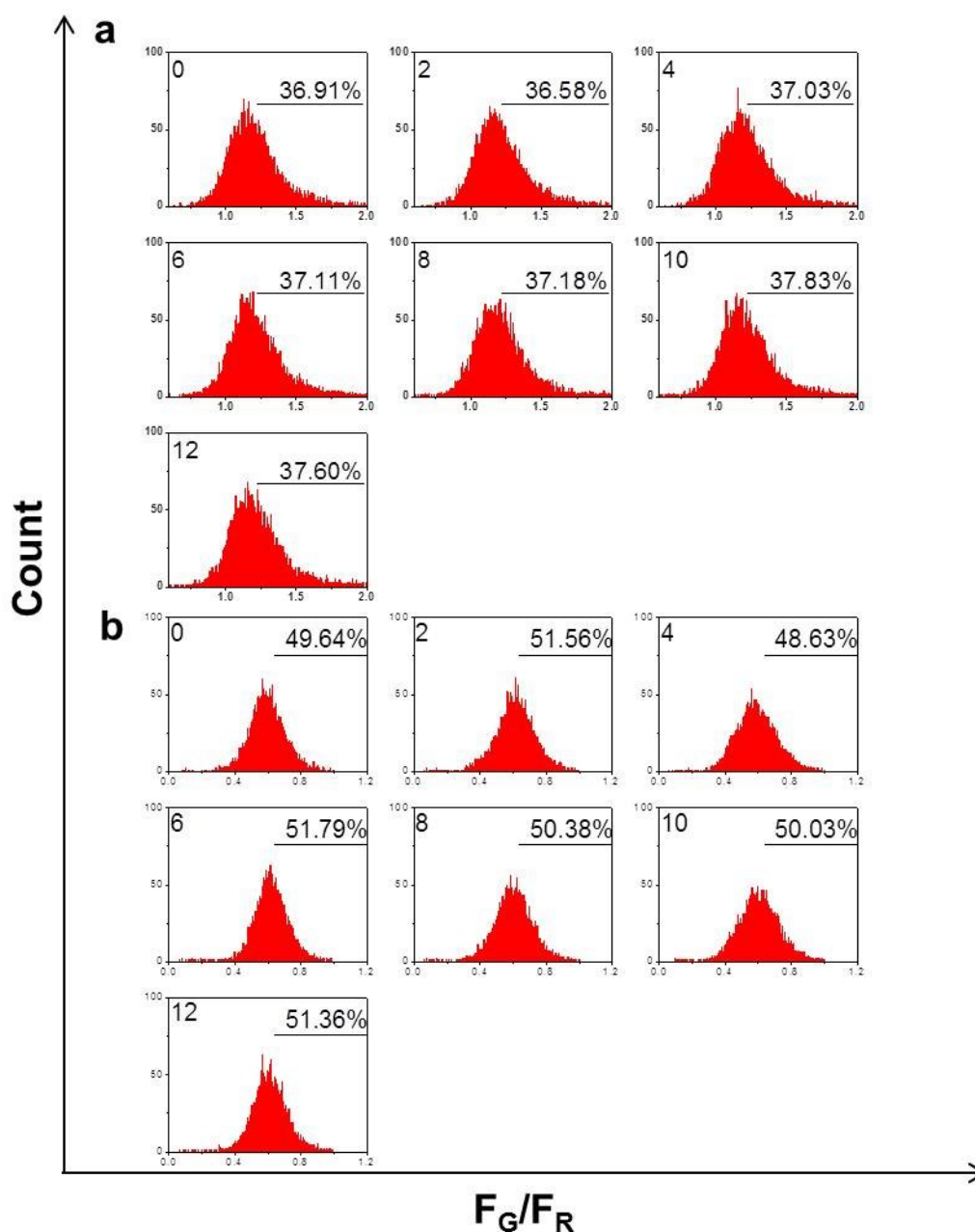


Fig. S25. Cell distribution pattern of MCF-7 (a) and SKOV3 (b) cells upon PBS (1×) incubation (37°C) determined in the dual channel ratiometric flow cytometric assay for intracellular endogenous labile Zn^{2+} according to the average F_G/F_R ratio (fluorescence ratio of green channel to red channel). Y-axis is the cell number; X-axis is the average F_G/F_R ratio. After being incubated with PBS for the desired time, the dissociated cells were stained with CPBT (10 μ M, 1 h) upon being cooled by ice, followed by rinse with PBS (1×). Then the flow cytometric assay was carried out with a dual channel mode (Green channel, 450 ± 25 nm; red channel, 570 ± 15 nm). λ_{ex} , 405 nm. $n \geq 3$, $p \leq 0.05$, cell number = 10000. The PBS incubation time was given along with the specific distribution pattern. The percentages indicate the proportion of cells with F_G/F_R higher than 0.6.

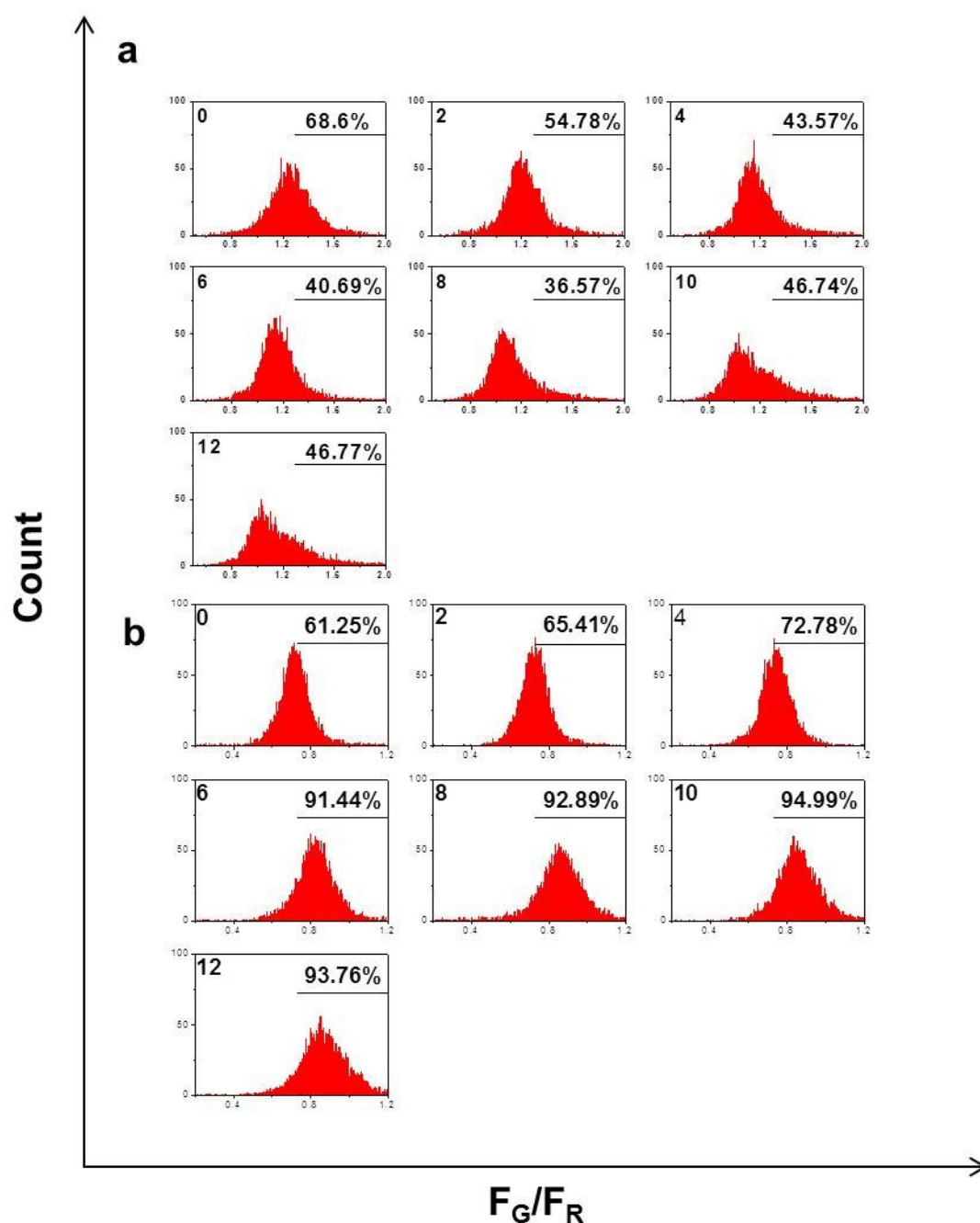


Fig. S26. Cell distribution pattern of MCF-7 (a) and SKOV3 (b) cells upon cisplatin (20 μ M, 37°C) incubation determined in the dual channel ratiometric flow cytometric assay for intracellular endogenous labile Zn^{2+} according to the average F_G/F_R ratio (fluorescence ratio of green channel to red channel). Y-axis is the cell number; X-axis is the average F_G/F_R ratio. After being incubated with cisplatin (20 μ M) for the desired time, the dissociated cells were stained with CPBT (10 μ M, 1 h) upon being cooled by ice, followed by rinse with PBS (1 \times). Then the flow cytometric assay was carried out with a dual channel mode (Green channel, 450 \pm 25 nm; red channel, 570 \pm 15 nm). λ_{ex} , 405 nm. $n \geq 3$, $p \leq 0.05$, cell number = 10000. The cisplatin incubation time was given along with the specific distribution pattern. The percentages indicate the proportion of cells with F_G/F_R higher than 0.6.

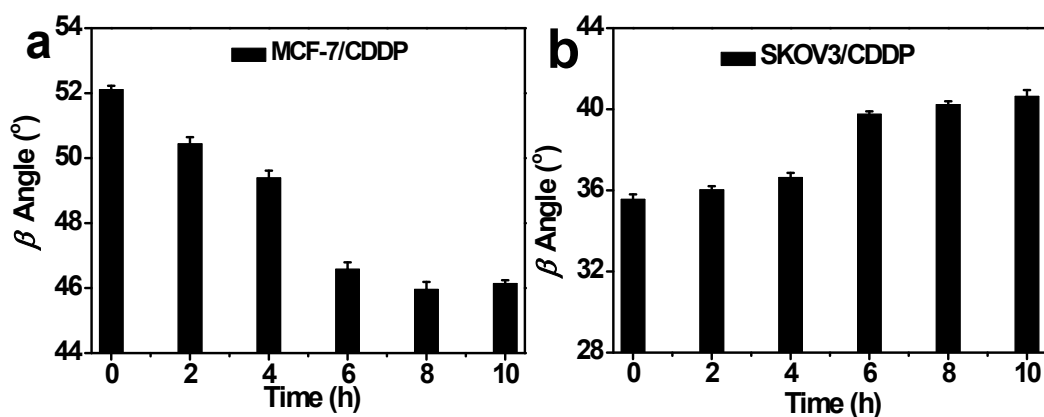


Fig. S27. Temporal profile of β angle for MCF-7 (a) and SKOV3 (b) cells after 0, 2, 4, 6, 8 and 10 h of cisplatin incubation. Error bars represent the SD $n \geq 3$.

7. Determination of chelatable $[Zn^{2+}]$ in cytoplasm of MCF-7 cells

The chelatable $[Zn^{2+}]$ in cytoplasm of MCF-7 cells was determined according to the following equation:

$$R = (R_{\min} K_d + R_{\max} [Zn^{2+}]) / (K_d + [Zn^{2+}]) \quad (\text{eq. 1})^4$$

R is the ratio of cytoplasm apparatus obtained in the ratiometric images. R_{\max} and R_{\min} are the ratios of cytoplasm apparatus after treated with $ZnCl_2$ /pyrithione (1:1) and TPEN solution respectively. K_d is the dissociation constant of CPBT/ Zn^{2+} complex obtained in Fig. S6. All the data are the average values according to 10 independent cells.

8. MTT assay of CPBT

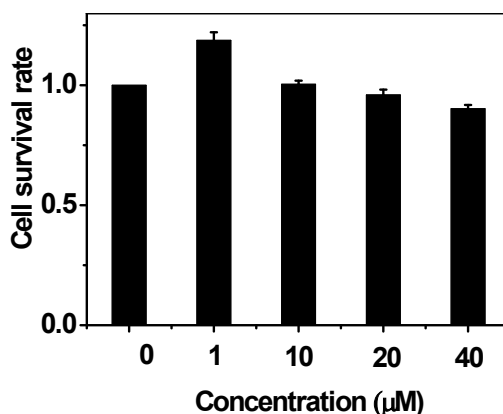


Fig. S28. Cell viability of MCF-7 cells treated with 0, 1, 10, 20 or 40 μM CPBT for 24 h.

References

1. Y. Chen, C. Zhu, J. Cen, J. Li, W. He, Y. Jiao and Z. Guo, *Chem. Commun.*, 2013, **49**, 7632.
2. M. Taki, J. L. Wolford and T. V. O' Halloran, *J. Am. Chem. Soc.*, 2004, **126**, 712.
3. C. Xu and W. W. Webb, *J. Opt. Soc. Am. B*, 1996, **13**, 481.
4. D. Atar, P. H. Backx, M. M. Appel, W. D. Gao and E. Marban, *J. Biol. Chem.*, 1995, **270**, 2473-2477.